Nuclear Materials Authority
P.O.Box 530 Maadi, Cairo, Egypt

GEOLOGY, GEOCHEMISTRY AND RADIOACTIVITY OF GABAL SHENDIB ALKALINE RING COMPLEX, SOUTH EASTERN DESERT, EGYPT

HASSAN A. A. SHAHIN and MASOUD S. MASOUD
Nuclear Materials Authority, P. O. Box 530, El-Maadi, Cairo, Egypt

ABSTRACT

Gabal Shendib alkaline ring complex forms high positive topographic rock units of concentric circular outcrop. The igneous complex has a diameter of 12 km emplaced within the metavolcanics and tonalite-granodiorite host rocks. The complex consists of olivine gabbro, alkaline granite, alkaline syenite and remnants of the volcanic rocks represented by porphyritic trachyte, porphyritic rhyolite, rhyolite and tuffs. These alkaline rocks show a strong enrichment in some rare metal contents (Zr = 4527, Nb = 717, Y = 806 ppm) and rare earth elements (La = 553, Ce = 1581, Pr = 214, Nd = 1145, Sm = 299, Gd = 55, Dy = 85ppm). The highest Rb/Sr ratio and lower Ba/Rb ratio of the studied alkaline rocks of Gabal Shendib ring complex indicating a high degree of fractionation of the melt associated with mineralization.

REE abundance patterns of the alkaline granite and alkaline syenite display M-type and W-type tetrad effect with strong Eu depletion in both whole rock samples. Fluid-melt interaction in the late stage of fractional crystallization is suggested to be the most important factor controlling the formation of REE tetrad effects in these alkaline rocks. The most important REE-bearing minerals are zircon, xenotime, monazite, allanite and apatite. Other accessory minerals include columbite, uranophane, urnothorite and titanite are identified.

Field radiometric measurements and chemical analysis for uranium content of the alkaline granite and alkaline syenite revealed low uranium content. Radioactivity level reaches up to 13.70 ppm eU in alkaline granite and 4.90 ppm eU in the alkaline syenite. Chemical analysis of uranium revealed that U content reaches up to 35 ppm in the alkaline granite and 15 ppm in the alkaline syenite.

INTRODUCTION

Several famous and known alkaline ring complexes in the Egyptian Deserts of the Pan-African orogenic belt, mostly circular alkaline complexes were emplaced in an intracontinental setting within the Arabian-Nubian Shield, which had been consolidated during the Pan-African orogeny (e.g., El-Ramly and Hussein, 1985; Harris, 1985; Vail, 1985a). Emplacement of the post-orogenic or inorogenic complexes in NE Africa took place during an extended period of time spanning almost the entire Paleozoic and Mesozoic Eras (Vail, 1990).

Many authors studied the structural setting of the Egyptian alkaline complexes (e.g. Bailey, 1964; Barberi et al. 1974; Black et al. 1985). The occurrence, tectonic environments and geochronology of the Egyptian alkaline ring complexes have been reviewed by several authors (e.g., El-Ramly et al., 1969,1970 and 1971; Hashad et al., 1979; DeGruyter and Vogel, 1981; Serencsits et al., 1981; E1-Ramly and Hussein, 1985). Several authors studied the peralkaline rocks in the Eastern Desert of Egypt, e.g. El-Reedy (1979) who studied the inorganic alkaline rocks in the south East-

ern Desert chronologically and proposed three phases of igneous activity, according to the Rb/Sr and K/Ar dates, they are 250-200 Ma, 155-125 Ma, and 110-70 Ma.

El Ramly and Hussein (1985) classified the ring complexes in the Eastern Desert on the basis of their magmatic differentiation, vaiety of rocks they include and on the degree of development of the ring nature into five groups namely, I) Abu Khruq type, II) Gezira type, III) Mishbeh type, IV) Mansouri type and V) Tarbite type. According to this classi-fication, Gabal Shendib ring complex belongs to the Abu Khruq type.

Abdallah (2006) studied the REE mineral-ized alkaline granites in Egypt. He divided the REE-mineralized alkaline granites in Egypt into three classes: (1) Mesozoic, anoro-genic nepheline syenite ring complexes with REE amounting up to 1.3 %, (2) anorogenic peralkaline syenite-granite, composed of i) Zr, Nb, REE, and Th-enriched peralkaline gran-ite-syenite complexes with REE amounting up to 0.5 % ii) Y, Th, HREE, and P-enriched post-Cretaceous   peralkaline complexes that intrude the Phanerozoic rocks of the south-Western Desert with REE amounting up to 2 % and (3) upper Proterozoic, post-orogen-ic siderophyllite alkaline granite with REE

amounting up to 0.8 %.

Gabal Shendib alkaline ring complex rep-resents one of the largest alkaline rocks in the south Eastern Desert. It is located at the southern extremity of the Eastern Desert of Egypt near the Sudan Frontier and occupies the southern half of Elba topographic sheet (NF-37 I),(Fig. 1). It lies at a distance of about 45 km south of Abu-Ramad city. It is bound by Lat. 21° 56' 40"-22° 06' 22" N and Long. 36° 10' 55"-36° 23' 12" E (Fig. 2).

Earlier authors, e.g. Ball (1912) studied the topography and geology of the south East-ern Desert, Egypt. Hume (1935) studied the fundamental Precambrian rocks of Egypt and Sudan. Takla et al., (1976) studied the tung-sten deposits in seven occurrences located in Eastern Desert of Egypt (Qash Amir-Elba, G. Homeirat, Um Bisilla, Abu Kharif, El Dob, Fatira, El-Bedia and Abu Hammad). They concluded that the ore is enclosed mostly with-in small younger granite intrusions, which are intruded into metamorphosed country rocks including metasediments, metavolcanics and amphibolite.

Hussein (1977) summarized the regional geology of the northern Red Sea in Egypt and in Sudan. He also carried out some detailed field, petrographical and geochemical works
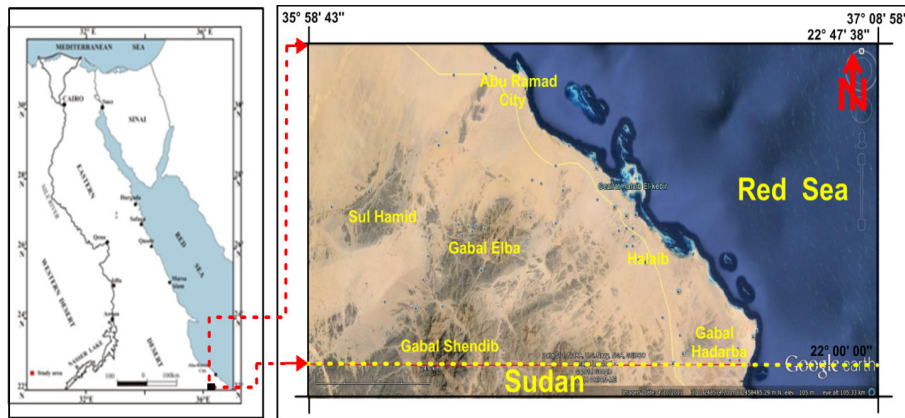

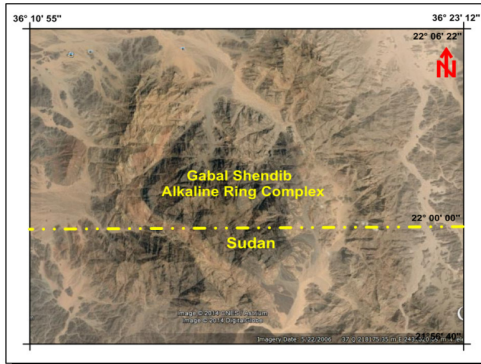Fig.1: Location map and Google image of the studied area

Fig.2: Close view of Google image for Gabal Shendib alkaline ring complex.

on the Sol Hamed complex and Halaib area. El-Alfy et al. (1994) geochemically explored the Elba-El Gerf area and he mentioned that there are a number of target areas that show anomalies of copper, nickel and chromium. Nasr and Youssef (1995) studied the Tertiary alkaline rocks in Gabal Elba area south Eastern Desert. They concluded that it may be Tertiary in age. El Agami et al. (1999) carried out mineralogical and geochemical studies on some mineralizaion in Halaib area, south Eastern Desert, Egypt. They concluded that the Mn-deposits of the granites and volcanic rocks in Halaib area are associated with tungsten and gold minerals, which were formed by hypogene hydrothermal solution.

Geological Survey of Egypt (1999) prepared geologic map on scale 1:250.000 for the basement rocks of Gabal Elba area between Lat. 22° 00'-23° 00'. According to this map Gabal Shendib ignous complex composed essentially of alkaline granite, syenite and rhyolite.

Ibrahim (1999) studied the tectonic evaluation and uranium potentiality of Elba ring complex, south Eastern Desert. He concluded that Elba ring complex forms a concentric semicircular pluton composed of extrusive and intrusive rocks. The extrusive rocks were originated from an alkaline to subalkaline magma by fractional crystallization process. The plutonic rocks are reversely zoned margin of alkaline granites through an internal zone of alkaline syenite to core of gabbro.

Shahin (2000) studied the geology, petrography and geochemistry of Gabal Elba area. He concluded that the mapped area is identified into four tectonostratigraphic assemblages, namely oceanic rocks, arc related rocks, late to post collision granites and within plate alkaline ring complex, as well as some minor sheet intrusions represented by dykes and veins. The oceanic rocks represented by metagabbros and metabasalts. The arc related rocks include metavolcanics and tonalite-granodiorite rocks. The syn to late orogenic granites are represented by alkaline feldspar-rich granites. The within plate alkaline ring complex forms the core of the Gabal Elba.

Darwish (2003) studied the petrographic, geochemical and spectrometric investigation of the rock units and their mineralization of Gabal Elba area and Gabal Shendib complex, south Eastern Desert. He concluded that the rock units of Gabal Elba area can be grouped into three tectonic-stratigraphic units, namely i) arc assemblage which include metavolcanics (meta-andesite to meta-rhyolite) and older granite (tonalite-granodiorite), ii) post-orogenic granites which include younger granites (monzogranite and alkaline feldspar granite), iii) alkaline ring complex which include volcanics and associated pyroclastics (andesite to rhyolite), gabbros, alkaline syenite and alkaline granite.

Ibrahim et al. (2006) studied the mineralogy, spectrometry and geochemistry of manganese ore in Halaib area, south Eastern Desert. They concluded that most of the manganese ore of Gabal Elba occurs as veins or fracture filling cutting across the structure of the host rocks (Miocene sedimentary and monzogranite) indicating epigenetic mineralization often in multi-stages. The ore of Gabal Elba is composed of pyrolusite, cryp-

tomelane and hollandite. They also concluded that the mineralization in Gabal Elba and Gabal Shendib represented mainly by secondary uranium (uranophane, beta-uranophane, kasolite and curite) and the associations (columbite, zircon, allanite, fluorite, zinwaldite and cassiterite).

Shahin (2014) study the Zr-Y-Nb-REE mineralization associated with microgranite and basic dykes at EL Sela shear zone, South Eastern Desert, Egypt. He concluded that these dykes hosting for uranium, rare metals (Zr, Y, Nb and Ga) and light rare earths (La, Ce, Sm and Nd) mineralizations.

This paper investigates principally the geology, geochemistry and radioactivity of Gabal Shendib alkaline ring complex, south Eastern Desert, Egypt.

GEOLOGIC SETTING

Gabal Shendib alkaline ring complex is a circular pluton reaching up to 12 km in diameter. The complex was emplaced within metavolcanics and tonalite-granodiorite host rocks. The outer part of the Shendib complex contains olivine gabbro, alkaline granite followed inwards by alkaline syenite. Remnants of the volcanic rocks represented by porphyritic trachyte, porphyritic rhyolite, rhyolite and tuffs occur in the southern part of the complex. A detailed geologic map was carried out on Gabal Shendib alkaline ring complex and the surrounding areas modified after Darwish (2003), (Fig.3).

Arc Related Rocks

Metavolcanics

The metavolcanics form a large extinction at Wadi Hareitra. These rocks range in color from dark green to grayish green color, massive, fine-grained, porphyritic, foliated, higly jointed and in some prats show highly schistose (Fig. 4). They are meta-andesite, meta-dacite and meta-rhyolite in composition. The associated meta-pyroclastics are of
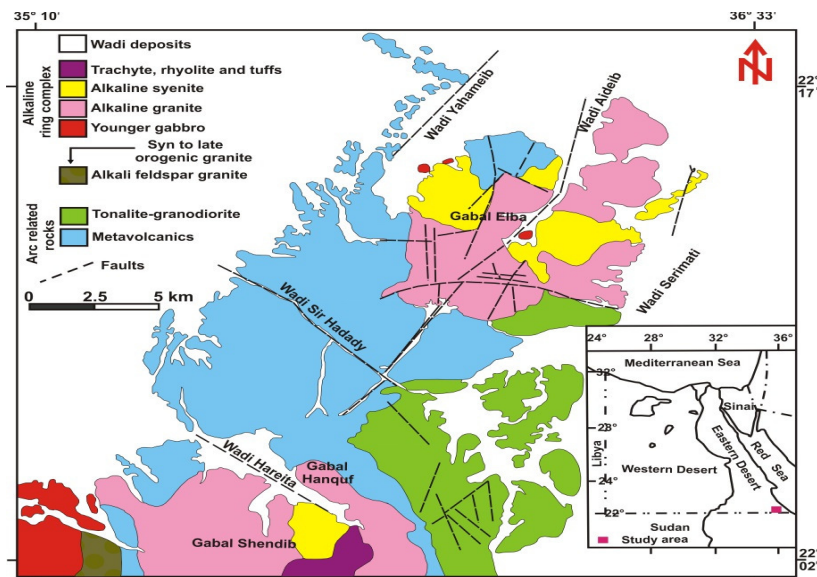

Fig.3: Geologic map of Gabal Shendib area, South Eastern Desert, Egypt (Modified after Darwish, 2003)

Fig.4: Photograph showing metavolcanic rocks at the front of Wadi Shendib, Looking SE

Fig.5: Photograph showing large xenoliths of pre-existing rocks in the granodiorite at Wadi Hiritra, Looking NW

minor occurrence and mainly represented by meta-agglomerates, banded meta-crystal tuffs and tuffs. Field relations indicate that they are intruded by tonalite-granodiorite, alkaline granite and alkaline syenite with sharp contact.

Tonalite-granodiorite

Tonalite-granodiorite are massive, hard and in some parts show highly deformed and highly weathered especially near the contacts. They are gray to dark gray in color, medium to coarse grained, highly jointed, characterized by cavernous, exfoliation and bouldery weathering and hosting xenoliths of pre-existing rocks (Fig.5). They are characterized by cavernous, exfoliation and boulder weathering. Field relations indicate that they are intruded the metavolcanics and intruded by alkaline granite and alkaline syenite with sharp contact.

Syn to Late Orogenic Granite

Alkali feldspar granite

The syn to late orogenic rock is represented only by the alkali feldspar granite. It is exposed in small outcrop south west of Gabal Shendib complex. It is pink to red in color,

medium to coarse-grained, highly weathered and highly jointed in some parts and massive in others. Field relation of this rock indicates that it intrudes the metavolcanics with sharp intrusive contact.

Alkaline Ring Complex

Younger gabbro

Younger gabbros form very small occurrences in the studied area. They are found as large xenolithic bodies in alkaline granite and alkaline syenite. It is medium to coarse grained, very hard and range in color from deep green to greenish black. In some places, they are fractured and show exfoliation, spherical to subrounded bouldary weathering forming onion shape (Fig.6). Field relation of this rock indicates that it is enclosed in the syenite at the end of Wadi Aideib and subround bouldery weathering enclosed in alkali granites at wadi Yahameib.

Alkaline granite

The alkaline granite forms considerable area at Wadi Shendib. It occupies a terrain of moderate to high relief at Wadi Shendib and is bounded from south west by the metavolcanics. It is massive, medium to coarse grained

Fig.6: Photograph showing exfoliation, spherical to subrounded bouldary weathering forming onion shape in younger gabbro at core of Wadi Aideib, Looking S
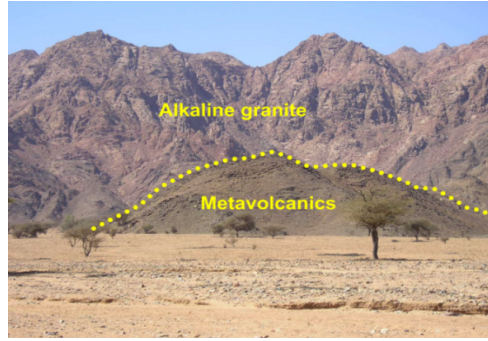

Fig.7: Photograph showing sharp contact between alkaline granite and metavolcanics, Looking SW

and ranges in color from pink to pinkish white. These rocks are highly weathered and jointed in some places. They are traversed by more than one set of joints, the first one is NE and dipping 80°/E and the second trending NW and dipping 60°/W. The alkaline granite shows a variable degree of weathering where in some places especially the high relief appears to be very massive whereas in other places especially the low relief appears to be highly weathered. Field relations reveal that it intrudes the arc related rocks with sharp intrusive contact (Figs.7&8) and intruded by alkaline syenite with sharp contact at Wadi Shendib (Fig.9).

Fig.8: Photograph showing sharp contact between alkaline   granite and tonalite-granodiorite, LookingW

Alkaline syenite

The alkaline syenite forms a small out-crops in the studied area, occupying the core of the Gabal Shendib ring complex. It forms high relief terrains, massive, medium to coarse grained and ranges in color from red-dish brown to red. This rock is highly jointed with NW direction and dipping nearly verti-cal.

Volcanic Rocks

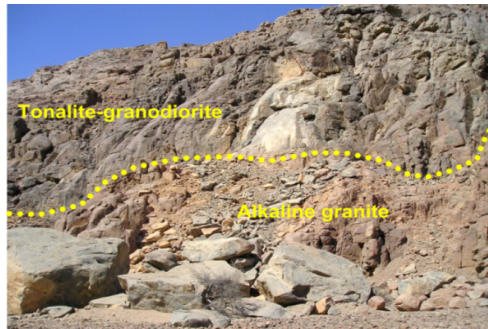The volcanic rocks in the studied area include porphyritic trachyte, porphyritic
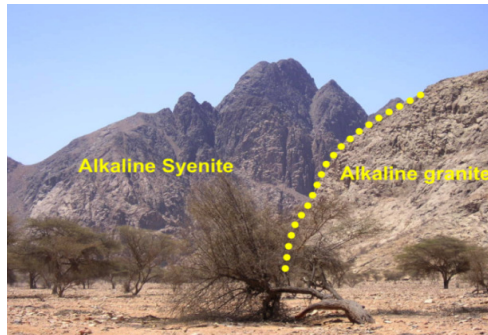

Fig.9: Photograph showing sharp contact between alkaline granite and alkaline syenite, Looking S

rhyolite, rhyolite and tuffs. The alkaline trachyte porphyry is pale gray rocks showing pronounced trachytic texture. The rhyolite is characterized by subhorizontal flows associated with welded tuffs, breccias and agglomerates. Field relations indicate that this rock extrudes the alkaline syenite with sharp contact at the end of Wadi Shendib (Fig.10).

PETROGRAPHY

Petrographically, Gabal Shendib alkaline complex is composed mainly of olivine gabbro, alkaline granite, alkaline syenite and remnants of the volcanic rocks represented by porphyritic trachyte, porphyritic rhyolite, rhyolite and tuffs. The olivine gabbro exhibits hypidomorphic granular texture. It is composed of plagioclase, olivine, pyroxene and secondary amphiboles as well as opaques. The alkaline granite is hypidiomorphic, equigranular, porphyritic, coarse-grained and pink to reddish pink color. Microscopically, it is composed essentially of alkali feldspar comprises orthoclase and perthite, quartz, alkaline amphibole (arvedsonite and riebeckite), minor plagioclase and biotite. The accessory minerals are zircon, apatite and iron oxides. Orthoclase occurs as megacrysts up to 5.4 x 2.2 mm. Most of the orthoclase crystals show

Fig.10: Photograph showing alkaline syenite extruded by porphyritic trachyte rock, Looking S

perthitic texture and still persevered the simple twinning (Fig.11). Perthite occurs as subhedral megacrysts up to 3.7 x 2.3 mm. Perthitic veinlets are the most predominate type of perthite in this granite (Fig.12). Quartz occurs as subhedral to anhedral small crystals up to 0.1 x 0.2 mm. It is found in two generations, the older fills the interstices between the K-feldspar crystals, whereas the younger appears as intergrowth with perthite crystals forming graphic and myrmeckitic textures (Figs.13&14). Arvedsonite and riebeckite represent the chief alkaline mafic amphibole minerals. It occurs as subhedral to anhedral crystals. It is characterized by its green color and strongly pleochroic (Figs.15&16).

The alkaline syenite of Gabal Shendib alkaline complex is composed essentially of alkali feldspars (orthoclase and perthite) and clots of alkali pyroxene. Under the microscope, the alkali feldspar occurs as tabular, euhedral to subhedral crystals (Fig.17). Aegirine augite is the chief mafic constituent occurs as subhedral tabular crystals (Fig.18). Some aegirine augite crystals show alteration to arfvedsonite and riebeckite (Figs.19&20). Sphene, apatite and opaques are accessory minerals.

The porphyritic rhyolite is composed of quartz and sanidine phenocrysts and laths of perthite orthoclase embedded in cryptocrystalline being composed of fine laths of quartz, sanidine, biotite, chlorite and iorn oxides (Fig. 21). The porphyritic trachyte is pale gray color showing trachytic texture. The rock is composed mainly of sanidine phenocrysts and laths of perthitic orthoclase. The groundmass is composed of perthitic orthoclase and small flakes of biotite (Fig.22).
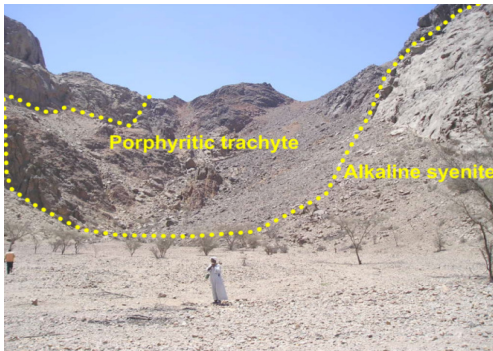
MINERALOGICAL INVESTIGATIONS

The mineralogical studies of the alkaline granite and alkaline syenite were performed on whole rock samples and separated mineral grains by petrographic microscope. Electron-Scanning Microscope (SEM) supported

Fig.11: Photo micrograph of orthoclase perthite showing simple twinning in the studied alkaline granite, XPL

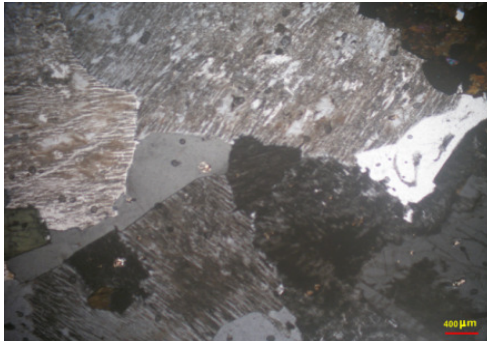Fig.14: Photomicrograph of myrmeckitic textures in the studied alkaline granite, XPL

Fig.12: Photomicrograph of perthite megacrysts showing perthitic veinlets in the studied alkaline granite, XPL
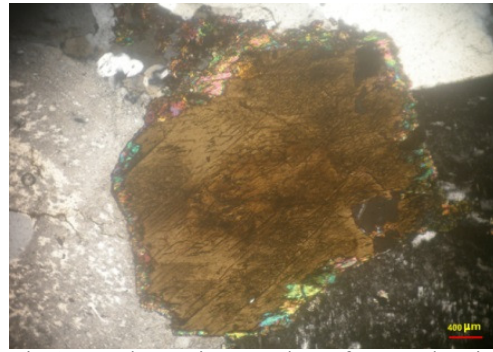

Fig.15: Photomicrograph of arvedsonite crystal with peripheral aegirine-augite in the studied alkaline granite, XPL
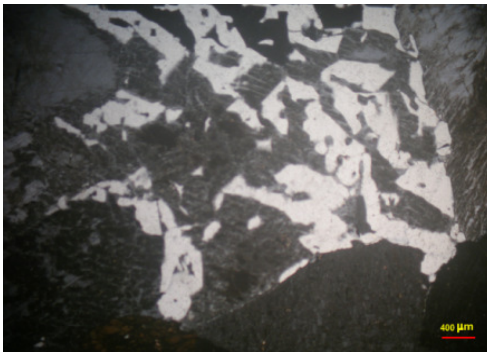

Fig.13: Photo micrograph of quartz and perthite crystal showing graphic texture in the studied alkaline granite, XPL
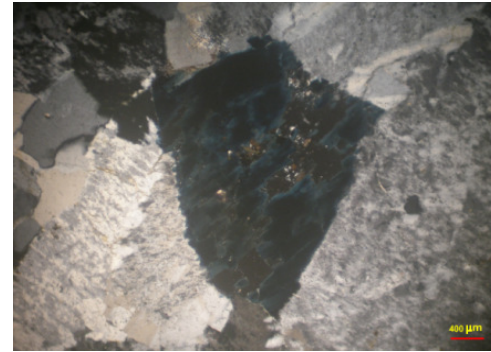

Fig.16: Photomicrograph of subhedral riebeckite crystal surrounded by perthite crystals in the studied alkaline granite , XPL

Fig.17: Photomicrograph of orthoclase perthite crystal showing simple twinning in the alkaline syenite, XPL
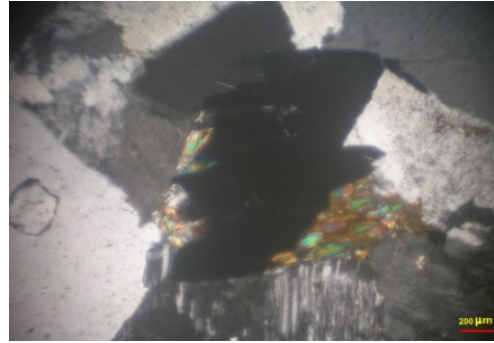

Fig.20: Photomicrograph of subhedral riebeckite crystal with peripheral aegirine-augite in the studied alkaline syenite, XPL
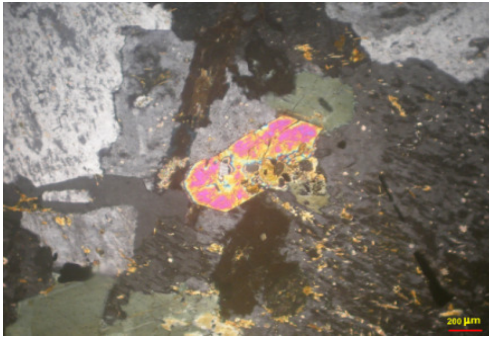

Fig.18: Photomicrograph of euhedral studied aegirine-augite crystal surrounded by perthite crystals in the alkaline syenite, XPL

Fig.21: Photomicrograph of orthoclase perthite showing simple twinning in the studied porphyritic rhyolite , XPL

Fig.19: Photomicrograph of subhedral crystal in arfvedsonite with perephral aegirine-augite in the studied alkaline syenite, XPL

Fig.22: Photomicrograph of euhedral sanidine phenocrysts showing trachytic texture in the studied porphyritic trachyte , XPL

by EDX. Scanning electron microscope (SEM) with a back-scattered electron imaging (BSE) of the alkaline rocks of Gabal Shendib ring complex show that these rocks host to a numerous small mineral occurrences include some rare metal contents (Zr, Nb, Y) and rare earths (La,Ce, Pr, Nd, Sm, Gd, Dy) elements. Radioactive minerals include uranophane and thorianite are also identified. Results of detailed mineralogical examination of these elements have been identified as follow:

Fig.24: EDS spectrum and BSE image of sodic feldspar coated by minute grains of uranophane

Uranophane

Uranophane is identified as individual anhedral grains in the studied alkaline granite, which range in color from lemon yellow to pale yellow. The most common impurity in this uranofane mineral is iorn oxide. Back-scattered electron (BSE) image of uranophane crystal showed uranophane crystal with matted intergrowth of minute fibers (Fig.23). Uranophane occurs as thin coatings on sodic feldspar minerals impling that the uranophane was added during the latest magmatic stage of the magma crystallization (Fig.24).

Urnothorite

Urnothorite occurs as individual minute grains up to 200 μm in size either as intergrowth with feldspars or inclusions in zircon in the studied alkaline granite (Fig.25).
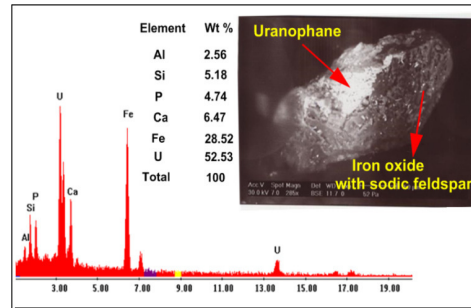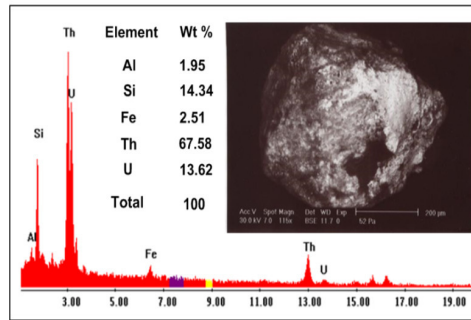

Fig.25: EDS spectrum and BSE image showing semi-quantitative chemical composition of urnothorite
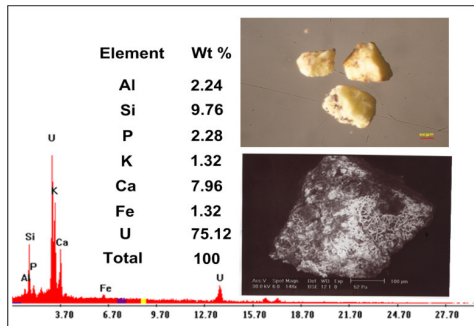
Fig.23: EDS spectrum, BSE image and photomicrograph showing semi-quantitative chemical composition of uranophane

Xenotime

Xenotime occurs as minute grains or as extremely thin coatings on zircon grains in the studied alkaline granite (Fig.26). The occurrence of xenotime at rim of zircon crystals implying that the xenotime was added during the latest magmatic stage of the magma crystallization.

Zircon

Zircon was found as the most abundant accessory mineral in the studied alkaline rocks of Gabal Shendib ring complex. Two types of zircon were distinguished from the studied sam-

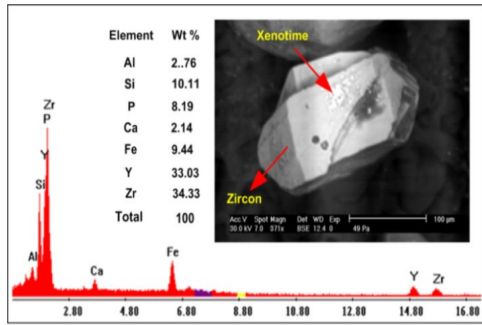Fig.26: EDS spectrum and BSE image showing semi-quantitative chemical composition of xenotime mineral coatings on magmatic zircon
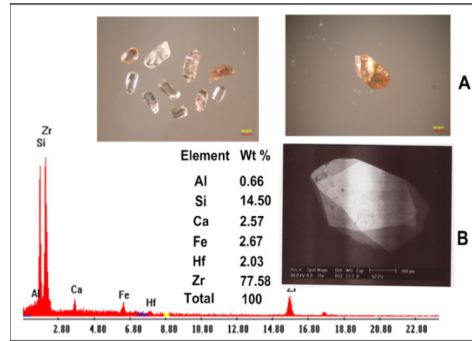

Fig.27: EDS spectrum, BSE image and photomicrograph showing semi-quantitative chemical composition of primary magmatic zircon

ples: primary magmatic zircon and metamict zircon. The magmatic zircon occurs in both alkaline rocks of Gabal Shendib as suhedral to euhedral prismatic colorless grains with bi-pyramidal terminations intergrown up to 200 µm in size (Fig.27). In the studied alkaline granite, zircon crystals are mainly characterized by considerable metamictization, due to the presence of uranium and thorium minerals (Fig.28). Scanning electron microscopy for zircon crystals revealed that xenotime occurs as minute grains or as extremely thin coatings on zircon grains (Fig.26).

Allanite

Allanite is an epidote-group mineral characterized by an abundant LREE, which can incorporate weight percents of the light rare earth elements (LREE) La, Ce and Nd. Back-scattered electron (BSE) image of allanite-shows minute grains or extremely thin coatings on the feldspar minerals of the studied alkaline syenite indicating that allanite was added during the latest magmatic stage of the magma crystallization (Fig. 29).

Monazite

Monazite is a phosphate mineral containing high percents of light rare earth elements (La, Ce). It occurs usually in small
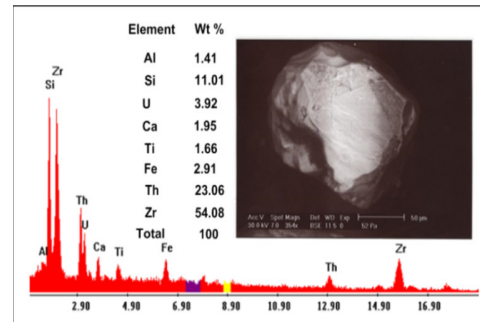

Fig.28: EDS spectrum and BSE image showing semi-quantitative chemical composition of metamict zircon
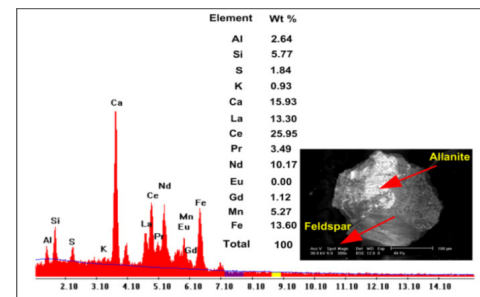

Fig. 29: EDS spectrum and BSE image showing semi-quantitative chemical composition of allanite coatings on feldspar grains

isolated crystals. Monazite is radioactive due to the presence of thorium and, less commonly, uranium, (Fig.30).

Ferrocolumbite

Ferrocolumbite grains were detected in the studied samples of the alkaline granite of Gabal Shendib alkaline ring complex. The grains are generally black in color with brilliant metallic luster under the transmitted light of an optical microscope. Th grains are usually characterized by the presence of U and Th (Fig.31).

Apatite

Apatite occurs in the form of massive, euhedral to subhedral grains with size up to 50µm in the studied alkaline rocks. The apatite crystals are generally light gray in color under the transmitted light of an optical microscope. Back-scattered electron (BSE) image of apatite showed two occurrence of apatite, the first one occurs as euhedral to subhedral primary magmatic grains (Fig.32), the second occurs as extremely thin coatings on the feldspar and quartz minerals, indicating that apatite was added during the latest magmatic stage of the magma crystallization (Fig.33).

Fig.31: EDS spectrum and BSE image showing semi-quantitative chemical composition of ferrocolumbite mineral

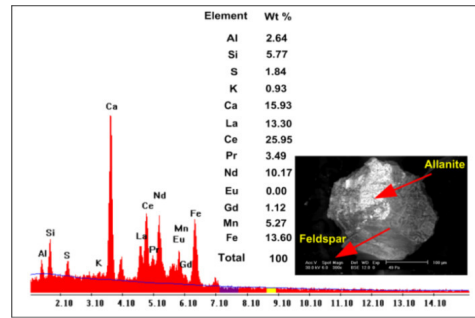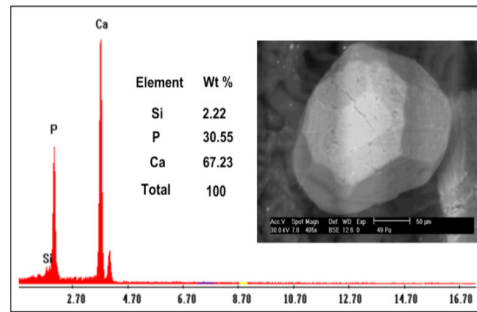Fig.32: EDS spectrum and BSE image showing semi-quantitative chemical composition of apatite
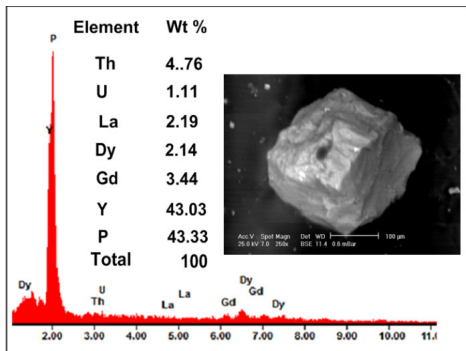

Fig.30: EDS spectrum and BSE image showing semi-quantitative chemical composition of monazite
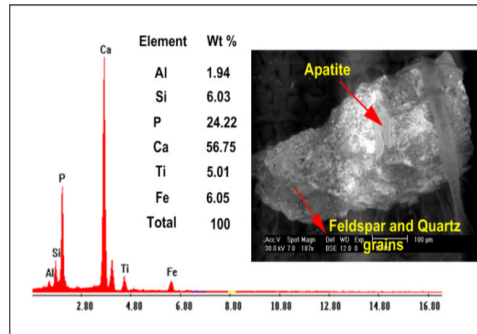

Fig.33: EDS spectrum and BSE image showing semi-quantitative chemical composition of apatite associated with feldspar and quartz minerals

Titanite

Titanite is one of the most common ac-cessory minerals occurring in   the studied alkaline rocks. It occurs as rod or rhombic crystals of size up to100μm (Fig.34).
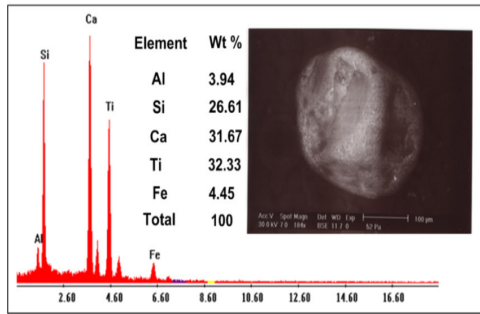
Fig.34: EDS spectrum and BSE image showing semi-quantitative chemical composition of titanite

RADIOMETRIC INVESTIGATION

Detailed field radiometric measurements using a portable four channel, gamma-ray spectrometer Model GR-230 was carried out along Gabal Shendib alkaline ring complex. The detailed field radiometric measurements revealed that low uranium content associated with alkaline granite and alkaline syenite. Radioactivity level was found to vary from 0.6 ppm to 13.7 ppm (eU) in alkaline granite and from 0.6 ppm to 4.90 ppm eU in alkaline syenite.

The statistical treatment of spectrometric data was expressed on binary diagrams of eTh versus eU, eU versus eU/eTh and eU ver-sus eU- eTh/3.5 (Fig. 35). Radiometric Data for alkaline granite and alkaline syenite are are listed in Table (1).

MATERIALS AND METHODOLOGY

Thirty samples from the fresh Gabal Shendib alkaline complex were collected for
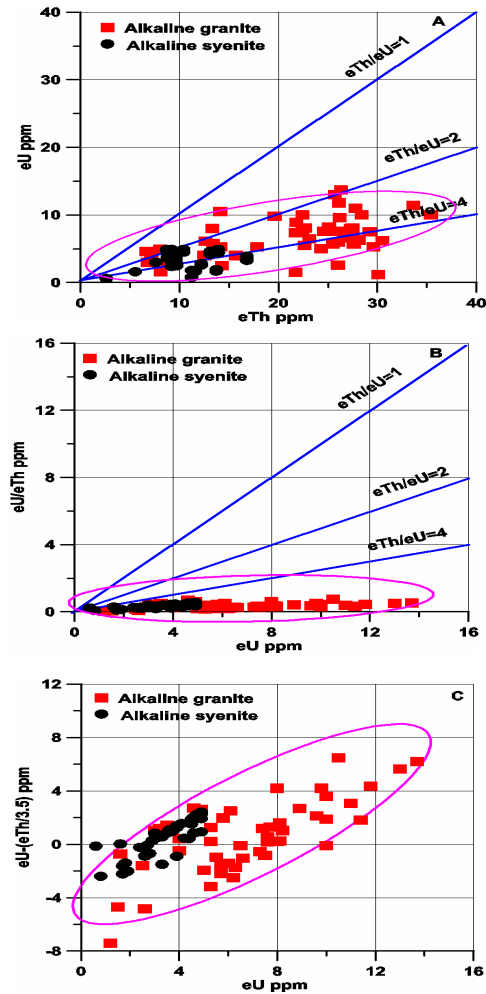
Fig. 35: Radioactive elements plot for ground gamma-ray spectrometry measurements for the studied alkaline   granite   and alkaline syenite A) eTh versus eU, B) eU versus eU/eTh and C) Mobility

Table 1: Radiometric measurements of the studied alkaline granite and alkaline syenite

Rock type	Total Count			K (%)			eU (ppm)			eTh (ppm)		
	Min.	Max.	Aver.	Min.	Max.	Aver.	Min.	Max.	Aver.	Min.	Max.	Aver.
alkaline granite (N=51)	17.60	48.20	33.34	1.70	7.50	5.12	0.8	13.70	6.15	4.00	35.40	19.60
Alkaline syenite (N=38)	12.70	32.30	25.29	3.30	6.50	5.15	0.6	4.90	3.32	2.60	16.80	10.07

this study. From these, twenty samples were selected for thin sections to study the mineral constituents of these granite and syenite. Ten samples were selected and chemically analyzed for their trace elements and REE by X-ray fluorescence analyzer (XRF) and inductively coupled plasma mass spectrometry (ICP- MS). The analyses were performed in the Nuclear Materials Authority Analytical Laboratories. Data of the trace elements and rare earth elements of the studied granite and syenite are listed in Tables (2&3).

GEOCHEMISTRY

Major and Trace Elements

The alkaline rocks of Gabal Shendib ring complex show high contents of Na_2O(4.5- 5.85%), K_2O (4.5- 5.98%) and low contents of CaO (1.02-1.70%), MgO (0.10-2.00%), Fe_2O_3(2.20-2.90%) and TiO_2 (0.66–.90%) , (Table 2).

SiO_2 versus K_2O diagram after Middlemost (1975) is used. This figure indicate that the most samples of the alkaline granite display medium-k to relatively high-k ,while the alkaline syenite show high potassium character (Fig. 36).

From the Al_2O_3/(CaO+Na_2O+K_2O) versus Al_2O_3/(Na_2O+K_2O) diagram, after Maniar and Piccoli (1989), (Fig. 37). It is indicating that the majority of samples have peralkaline characters. From the Agpaitic index (AI = Na + K/Al) versus SiO_2 diagram, the majority of samples have agpatic index (AI = Na + K/Al) > 1 (Fig. 38) and are thus classified as peralkaline granites according to Lie´geois and Black (1987). On the (Na + K)/Al versus Zr (ppm) diagram of the peralkaline plutons (Fig. 39), after Shellnutt & Zhou (2007) and Shellnutt et al. (2009a), most of the studied samples occur in the peralkaline field. The K-Rb diagram (Fig. 40) shows that the magmatic trend (1000-100 MT) is given by Shaw

Table 2 : Major oxides (wt. %) and trace element data (ppm) of the studied alkaline granite and alkaline syenite rocks

S. No.	Alkaline granite					Alkaline syenite				
	Sh2	Sh6	Sh9	Sh10	Sh13	Sh5	Sh7	Sh8	Sh12	Sh14
SiO_2	71.40	70.10	70.40	69.9	70.3	55.20	58.40	56.30	58.00	54.80
TiO_2	0.66	1.90	0.63	0.65	0.75	1.02	0.12	1.06	1.03	1.06
Al_2O_3	12.13	12.20	12.65	12.4	12.4	16.65	16.50	16.25	16.35	16.50
Fe_2O_3	2.60	2.20	2.23	2.80	2.90	2.70	2.42	2.54	2.63	2.45
MnO	0.26	0.70	0.30	0.42	0.21	0.70	0.40	0.50	0.65	0.90
MgO	2.00	0.10	0.55	0.30	0.45	0.60	0.55	0.40	0.50	0.56
CaO	1.04	1.02	1.08	1.7	1.08	1.20	1.40	1.35	1.22	1.30
Na_2O	4.60	4.70	4.65	4.50	4.40	5.50	5.85	5.75	5.65	5.20
K_2O	4.50	4.80	4.72	4.6	4.7	5.90	5.98	5.95	5.93	5.70
P_2O_5	0.01	0.08	0.11	0.12	0.13	0.06	0.03	0.08	0.04	0.08
LOI	0.80	0.80	0.30	0.31	0.33	2.10	1.20	0.29	0.40	0.80
Total	100	١٠٠	99.40	99.69	100	99.28	100.03	100.29	100.07	100
A/CNK	0.81	0.79	0.82	0.78	0.83	0.89	0.85	0.85	0.87	0.92
A/NK	0.89	0.86	0.91	0.92	0.92	0.98	0.94	0.93	0.95	1.02
Trace elements (ppm)										
Cr	28	35	68	31	30	89	139	196	106	38
Ni	6	8	4	7	11	9	5	4	4	11
Cu	10	10	10	11	12	10	16	11	9	9
Zn	73	136	77	74	79	124	181	124	71	95
Zr	816	1303	666	680	809	1510	987	1544	723	4527
Rb	49	151	133	127	78	148	64	158	112	78
Y	493	806	296	415	497	665	320	498	235	270
Ba	95	83	79	98	88	317	280	310	282	290
Pb	9	8	11	7	12	11	58	26	11	9
Sr	29	46	24	25	29	54	8	7	8	11
Ga	25	22	6	24	23	6	113	63	12	41
V	3	3	14	12	20	7	333	12	51	621
Nb	110	138	137	144	130	275	142	222	104	717
U	10	35	15	8	5	7	10	15	7	8
K/Rb	762	264	295	301	500	331	776	313	440	607
Rb/Sr	1.69	3.28	5.54	5.08	2.69	2.74	8.00	22.57	14	7.09

Note: A/CNK = molar ratio of Al_2O_3/(CaO + Na_2O + K_2O), A/NK = molar ratio of Al_2O_3/(Na_2O + K_2O)
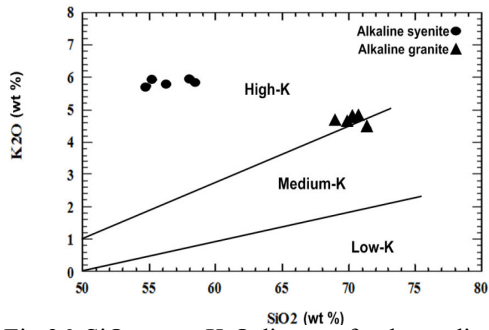
Fig.36: SiO₂ versus K₂O diagram for the studied alkaline rocks, after Middlemost (1975)
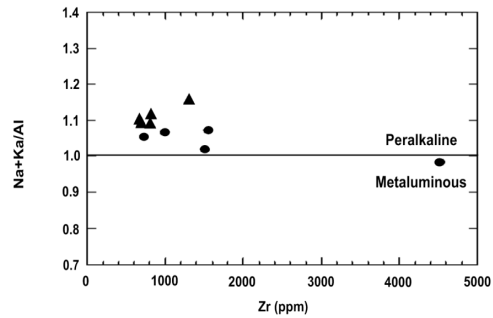

Fig.39: (Na + K)/Al versus Zr diagram of the peralkaline plutons. Data from Shellnutt & Zhou, (2007) and Shellnutt et al. (2009a), (Symbols as on Fig. 36)
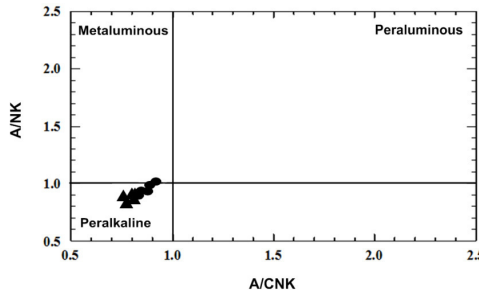

Fig.37: Shand's index diagram for studied alkaline rocks of Gabal Shendib ring complex. Fields after Maniar and Piccoli (1989), (Symbols as on Fig. 36)
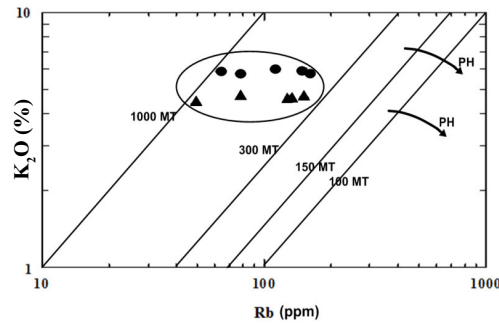

Fig.40: K-Rb variation diagram for the studied alkaline rocks of Gabal Shendib ring complex (After Shaw, (1968), crustal K/Rb ratio (After Taylor, (1965), (Symbols as on Fig. 36)
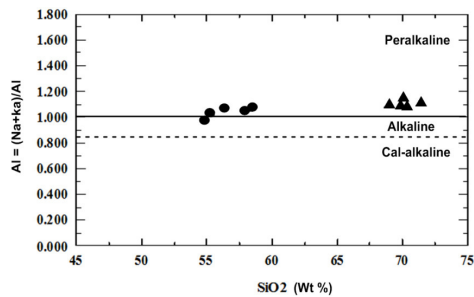
Fig.38: Agpaitic index (AI=Na+K/Al) versus SiO₂ diagram showing the alkaline to peralkaline characters of the studied alkaline rocks. Note that the line with AI = 0.87 (Lie´geois and Black, 1987) separates alkaline and calc-alkaline granite series (Symbols as on Fig. 36)

(1968), while the average crustal K/Rb ratio is 250 (Taylor, 1965). The alkaline granite and alkaline syenite of Gabal Shendib ring complex samples plotted between the magmatic trend (300-1000 MT) is given by Shaw (1968) and near the average crustal K/Rb 250 of Taylor (1965). The computed K/Rb ratio decreases from the alkaline syenite (776 ppm) to the alkaline granite (264 ppm). The lower K/Rb ratios in the alkaline syenite indicate more differentiated and more evolved magmatic liquids.

From the K-Ba variation diagram of Ma-

son, (1966) who is determine the crustal average ratio (K/Ba=65), the plot of the studied alkaline granite and alkaline syenite samples occur above the average crustal ratio with K/Ba ratio (>65), showing Ba depletion with K_2O enrichment which indicates highly fractional crystallization lead to the enrichment of K_2O in residual melts (Fig.41). Early precipitation of Ba is reciprocal to the behavior of Rb, and the Ba/Rb ratio rates as one of the most sensitive indicators of fractionation (Taylor &Heier 1960; Taylor,1963). The Rb-Ba variation diagram of Mason (1966) shows that Ba is depleted

relative to Rb (Fig. 42). According to this diagram the studied alkaline granite and alkaline syenite samples are plotted around the average crustal values ranging between (4.4 and 0.44) which indicate high evolution of magma and crystal-melt fractionation. The Rb versus Sr diagram (Fig.43), indicate that the studied alkaline rocks consistent dominantly with alkali feldspar fractionation indicating a good agreement with their hypersolvus character and the predominace of perthites and higher proportion of alkali feldspar fractionation required to evolve the peralkaline rocks of Gabal Shendib ring complex.

Rare Earth Element Geochemistry

The concentration of ΣREE in the studied alkaline rocks show a significant variation (range from 215 ppm to 4027 ppm and an average of 1211 ppm). Two distinct groups are differentiated: I. REE-relatively rich group with total REE<337 ppm which includes the alkaline syenite samples, II. REE-highly rich group with ΣREE up to 4027 ppm which includes the alkaline granite samples (Table 3). The REE-relatively rich group (Group I) displays chondrite-normalized pattern (Fig. 44) with weak to moderate LREE/HREE fractionation (6 to 11) and a moderate negative Eu anomaly (Eu/Eu*≈0.2– 0.4). The REE-highly rich group (Group II), on the other hand,

Fig.41: K-Ba variation diagram for the studied alkaline rocks of Gabal Shendib ring complex, average crustal ratio (After Mason, 1966), (Symbols as on Fig. 36)

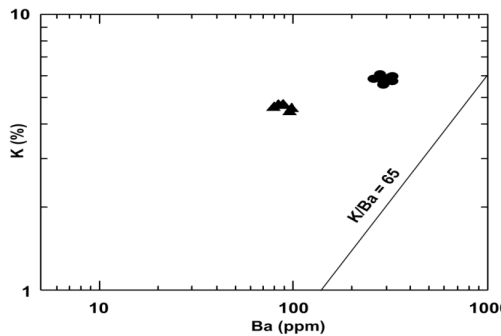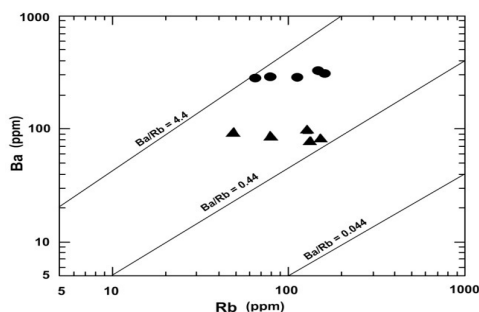Fig.42:Rb-Ba variation diagram for the studied alkaline rocks of Gabal Shendib ring complex(After Mason, 1966), (Symbols as on Fig. 36)
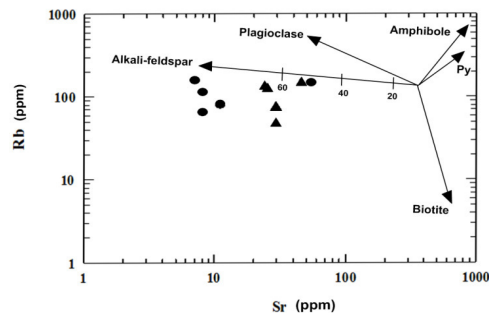

Fig. 43: Sr versus Rb variation diagram for the studied alkaline rocks of Gabal Shendib ring complex (After Mason,1966), symbols as on Fig.36

Table 3: Rare earth element constituents (ppm) of the studied alkaline granite and alkaline syenite

S.No.	Alkaline granite			Alkaline syenite			
	Sh6	Sh9	Sh13	Sh5	Sh7	Sh8	Sh12
La	33.39	19.61	553.00	63.07	37.77	34.48	36.50
Ce	82.50	46.79	1581.35	193.39	116.63	83.06	82.89
Pr	13.18	5.92	214.94	27.48	17.12	10.49	10.28
Nd	70.22	2782	1145.33	153.35	89.78	50.38	46.82
Sm	18.34	9.80	299.74	42.32	23.92	16.23	12.67
Eu	1.24	1.11	4.63	1.87	3.06	1.53	0.85
Gd	8.63	7.70	55.65	12.46	19.70	15.20	7.30
Tb	1.48	1.32	16.47	2.33	3.29	2.15	1.25
Dy	7.69	8.00	85.94	16.40	16.66	9.29	7.06
Ho	1.96	1.74	24.15	2.65	2.65	1.82	1.99
Er	3.40	3.37	36.54	5.28	4.85	3.23	4.65
Tm	0.60	0.39	2.75	0.81	0.62	0.48	0.45
Yb	2.73	2.00	3.74	3.74	1.94	2.18	2.16
Lu	1.08	0.46	2.48	0.70	0.22	0.72	0.29
LREE	219	2865	3799	481	288	196	190
HREE	28	25	228	44	50	35	25
ΣREE	246	2890	4027	526	338	231	215
LREE/HREE	8	115	17	11	6	6	8
Eu/Eu*	0.3	0.4	0.1	0.2	0.4	0.3	0.2
Ce/Ce'	0.922	0.219	1.072	1.090	1.106	1.015	0.999
Pr/Pr'	1.001	0.046	0.996	1.003	1.059	0.984	0.993
(La/Yb)cn	8.3	6.6	99.9	11.4	13.2	10.7	11.4
(Tb/Yb)cn	2.3	2.8	18.8	2.7	7.3	4.2	2.5
(Gd/Yb)cn	2.6	3.1	12.0	2.7	8.2	5.6	2.7
(La/Sm)cn	1.1	1.3	1.2	0.9	1.0	1.3	1.8
Tm/Tm'	0.968	0.841	0.690	1.126	1.341	0.917	0.913
Yb/Yb'	0.495	0.643	0.177	0.783	0.903	0.527	0.848
t1	1.00	0.10	1.03	1.05	1.08	1.00	1.00
t3	0.90	1.00	1.12	1.17	1.11	0.92	0.85
t4	0.70	0.70	0.35	0.94	1.10	0.70	0.90
TE1,3	0.90	0.30	1.07	1.11	1.10	0.961	0.92
TE1,4	0.80	0.30	0.60	0.99	1.10	0.834	0.94

shows moderately to highly fractionated chondrite-normalized pattern (Fig.45) with LREE/HREE ratios range from 8 to 115 and negative Eu anomaly (Eu/Eu*≈0.1–0.4) similar to the first group.

REE Tetrad Effect

The term 'tetrad effect' in geochemistry refers to the subdivision of the 15 lanthanide elements into four groups in a chondrite normalized distribution pattern: (1) La–Ce–Pr–Nd, (2) Pm–Sm–Eu– Gd, (3) Tb–Dy–Ho and (4) Er–Tm–Yb–Lu, and each group forms a smooth convex (M-type) or concave (W-type) pattern (Masuda et al.,1987). The values of tetrad effect were calculated according to the quantification method of Irber (1999):t1 = (Ce/Ce*× Pr/ Pr*), t3 = (Tb/Tb*×Dy/Dy*), t4 =(Tm/Tm* ×Yb/Yb*), Degree of the tetrad effect T1,3 = (t1 × t3)0.5.

In most geological samples the chondrite-normalized REE abundances form a smooth linear or curvilinear trend, which is the famous Masuda-Coryell diagram (Henderson, 1984; Rollison, 1993). Masuda and Ikeuchi (1979) first found the W-type REE tetrad effect in various marine materials, including
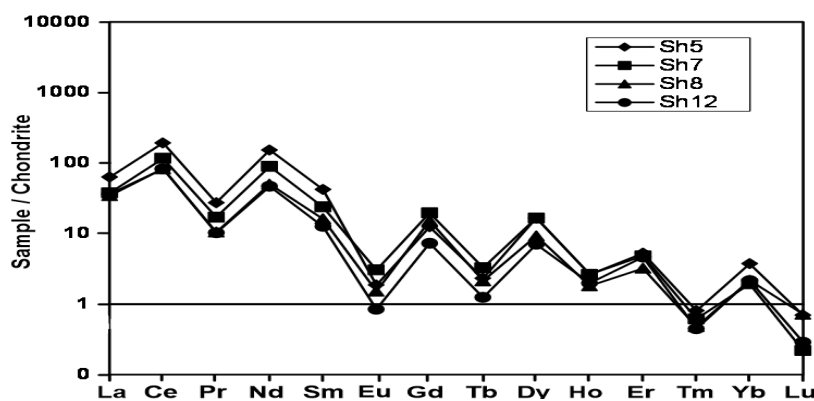

Fig. 44: Chondrite-normalized REE pattern for the alkaline syenite of Gabal Shendib ring complex. The chondrite values for the normalization are from Boynton (1984)
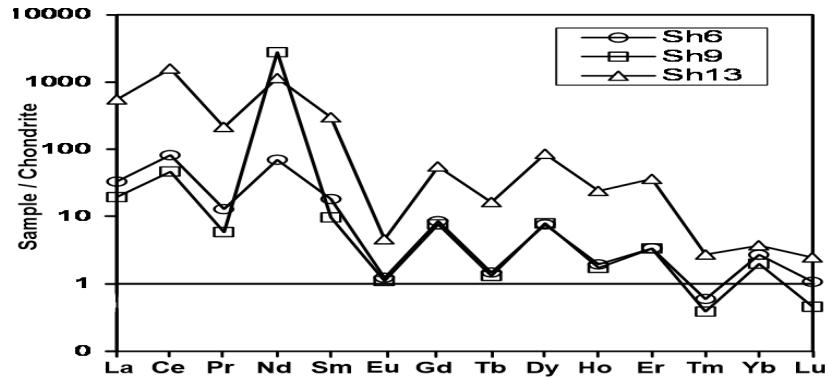
Fig. 45: Chondrite-normalized REE pattern for the alkaline granite of Gabal Shendib ring complex. The chondrite values for the normalization are from Boynton (1984)

sea water, algae, sponges, shells limestones, etc., and soon afterwards, they found similar REE distribution feature in groundwater. Masuda et al. (1987) and Zhao (1988,1992) found the M-type REE tetrad effect in rare-metal granites of South China. Bau (1996) and Irber (1999) also found the same feature in granites of Egypt and Germany. Ratios, such as $(La/Yb)_N$, $(La/Sm)_N$, $(Gd/Yb)_N$ and Eu/Eu*, Ce/Ce* can provide important petrogenetic and metallogenic information (Schi1ling, 1975; Jahn et al., 1982; Frey, 1984; Rollison, 1993).

Chondrite-normalized   pattern   (Fig.44) shows that alkaline syenite sample (Sh5) has strong M-type tetrad effect in the third tetrad effect, while sample (Sh12) show strong W-type tetrad effect in the third tetrad effect (Table 3), suggesting changes in physicochemical conditions that prevailed during hydrothermal alteration of these rocks.

Chondrite-normalized   pattern   (Fig.45) shows   that all samples of alkaline granite and one sample of alkaline syenite (Sh8) have strong W-type tetrad effect in the fourth tetrad effect Table (3). The index of tetrad effect intensity, $TE_{1,3}$, is higher than 1.10 in one sample of alkaline syenites. On the other hand, the index of tetrad effect intensity, $TE_{1,4}$, is lesserr than 0.9 in all samples of alkaline granites

ranging from 0.3 to 0.8 and one sample (Sh8) in alkaline syenite reach up to 0.83 which implies that there was   an interaction between melt and   water-haloid-rich fluid when these rocks are crystallized from magma.

CONCLUSIONS

The alkaline rocks of Gabal Shendib ring complex are composed of olivine gabbro, alkaline granite, alkaline syenite and remnants of the volcanic rocks represented by porphyritic trachyte, porphyritic rhyolite, rhyolite and associated pyroclastics. Distribution of mineralization in the alkaline rocks indicate a post-magmatic hydrothermal fluides. These alkaline rocks provided a source for the mineralizing elements such as Zr, Y, Nb, Th, U and REE. Geochemical variation of Rb/Sr and Ba/Rb ratios indicate variable degree of fractionation trend in the Gabal Shendib complex magma.   The highest Rb/Sr ratio and lower Ba/Rb ratio indicate to alteration processes and high degree of fractionation. The behaviors of Rb, Ba and Sr suggest that the development of volatile-rich residual fluids in Gabal Shendib complex magma. Chondrite-normalized REE pattern   for the alkaline rocks of Gabal Shendib ring complex display

M-type and W-type tetrad effect and strong Eu depletion in both whole rock samples indicating fluid-melt interaction, enrichment of volatile, alkaline, rare earth elements and rare metals (Zr, Y, Nb, U) in the late stage of fractional crystallization.

REFERENCES

Abdallah, H.M, 2006. An Overview on the REE mineralized Alkaline Granites in Egypt, with Special Reference to the Abu Khruq and Gara El Hamra Bodies. Resource Geology, 56, no.3, 365-370.

El Agami, N.L.; Abu Baker, M. A.;Ibrahim, M. E., and Rashed, M.A., 1999. Mineralogical and geochemical studies on some mineralization in Halaib area, south Eastern Desert, Egypt. J. Geol., 43/1, 27-34.

Abu Elatta, S.A. ; Assran, H.M., and Ahmed, A. A., 2013. Preliminary Study on HFSE Mineralization in the Peralkaline Granites of Nusab El Balgum Area, South Western Desert, Egypt. Geomaterials, 3, 90 -101.

Bailey, D.K., 1964. Crustal warping.A possible tectonic control of alkaline magmatism. J. geophys. Res'., 69, 1103-1111.

Ball, J., 1912. The geography and geology of south eastern Egypt. Geol. Surv., Cairo, 394p.

Barberi, F.; Bonatti, E.; Marinelli, G., and Varet, J., 1974. Transverse tectonics during the split of a continent: data from the Afar rift. Tectonophysics, 23, 17-29.

Bau, M., 1996. Controls on the fractionation of isovalent trace elements in magmatic and aqueous systems: evidence from Y/Ho, Zr/Hf and lanthanide tetrad effect. Contrib. Mineral. Petrol., 123, 323–333.

Black, R.; Lameyer, J., and Bonin B., 1985. The Structural Set-ting of Alkaline Complexes, J. Afri. Earth Sciences, 3, No. 1-2, 5-16.

Darwish, M.S., 2003. Geochemical, mineralogical and radioactive studies in Elba area, south Eastern Desert, Egypt. Ph. D. Thesis, Fac. Sci., Mansoura Univ., Egypt, 261p.

DeGruyter, P.D.; Vogel, T.A., 1981. A model for the origin of the alkaline complexes of Egypt. Nature 291, 571-574

El Alfy, Z.; Bagddady, M.; Awaga, G.; Morsei, A.; Ramadan, T., and Abdallah, M. A., 1994. Geochemical exploration of Elba – Gerf area south Eastern Desert, Egypt, Geol. Surv. , Cairo (unpublished report).

El Ramly, M. F.; Budanov, V. I.; Armanious, L. K., and Dereniuk, N. E., 1969. The three ring complexes of Gabal El Kahfa, GabalNigrub El Fogani and Gabal El Naga, south Eastern Desert of Egypt. Geol. Surv. Egypt, paper No. 52, 39 p.

El Ramly, M.F.; Budanov, V.I.; Hussein, A. A., and Dereniuk, N.E., 1970. Ring complexes in the south Eastern Desert of Egypt. In: Studies of some mineral deposits of Egypt, (Osman Moharam et al., Eds.), Geal. Surv. Egypt , 181-194.

El Ramly, M.F.; Budanov, V.I., and Hussein, A. A., 1971. The alkaline rocks of south Eastern Desert, Egypt. Geol. Surv. Egypt, Paper no. 53.

El-Ramly, M.F; Hussein A.A.A., 1985. The ring complexes of the Eastern Desert of Egypt. J. Afr. Earth Sci., 3, 77-82.

El Reedy, M.W.M., 1979.Geochronological and geochemical studies on the alkalinec rocks in the South Eastern Desert, Ph. D. Thesis, Fac. Sci., Cairo Univ., 290p.

Egyptian Geological Survey, 1999. The basement rocks of Gabal Elba Quadrangle, Scale, 1:250,000. Geol. Surv. Egypt, Cairo.

Frey, F.A., 1984. Rare earth element abundances in upper mantle rocks. In: Rare Earth Element Geochemistry (Henderson, P., Ed.). Developments in Geochemistry, 2, 153–192.

Harris, N.B.W., 1985. Alkaline complexes from the Arabian Shield. J. Afr. Earth Sci., 3, 83-88.

Hashad, A. H., and El Reedy, M.W.M., 1979. Geo-

chronology of the anorogenic alkaline rocks, south Eastern Desert, Egypt. Ann. Geol. Surv. Egypt, 9, 81-101.

Henderson, H., 1984. General geochemical properties and abundances of the rare earth elements. In: Rare Earth Element Geochemistry (Henderson, P., Ed.). Develpoments in Geochemistry, 2, 1–9.

Henderson,H., 1996. Rare earth elements, introduction and review. In: Rare earth minerals:Chemistry, origin and deposits (Jones, A.P.; Wall, F. and Williams, C.T., Eds.). The Mineralogical Society Series, 1-19.

Hume, W.F., 1935. Geology of Egypt. II. The fundamental Precambrian rocks of Egypt and Sudan : Part I, The metamorphic rocks : 1 – 300, Part II, The later plutonic and minor intrusive rocks : 301- 688, Part III, The minerals of economic value : 689 – 900. Geol. Surv. Egypt.

Hussein, I. M., 1977.Geology of the Halaib area of the northern Red Sea Hills, Sudan, with reference to the Sol Hamed basic complex. M. Sc. Thesis, Portsmouth Polytechnic, England.

Ibrahim, M. E.,1999. Tectonic evolution and uraium potentiality of Elba ring complex, south Eastern Desert, Egypt. Egyptian Mineralogist, 11, 39-62.

Ibrahim, M.E.; Saleh, G.M.; Darwish, M.S., and Khalaf, M. A., 2006. Mineralogy, spectrometric investigations and geochemistry of manganese ore in Halaib area, south Eastern Desert. 7th Inter. Conf. Geochem., Alexandria, Egypt.

Irber, W., 1999. The lanthanide tetrad effect and its correlation with K/Rb, Eu/Eu*, Sr/Eu, Y/Ho and Zr/ Hf of evolving peraluminous granite suits. Geochim. Cosmochim. Acta, 63, 489–508.

Irvine, T.N., and Baragar, W.R.A., 1971. A guide to the chemical classification of the common volcanic rocks. Canadian J. Earth Sci., 8, 523 – 548

Jahn, B. M.; Gyuau, G., and Glikson, A., 1982. Komatiites of the overwacht group, S. African: REE geochemistry, Sm/Nd age and mantle evo-

lution. Contrib. Mineral. Petrol., 80, 25–40.

Lie´geois, J.P., and Black R., 1987. Alkaline magmatism subsequent to collision in the Pan-African belt of the Adrar des Iforas (Mali). In: Alkaline igneous rocks (Fitton JG., Upton, BJG., Eds). J Geol. SocLond, Special Publication, 30, 381–401

Maniar, P. D., and Piccoli, P. M., 1989. Tectonic discrimination of granitoids. Geol. Soci. Am. Bull., 101, 63 5-643.

Mason, B., 1966. Principles of geochemistry. 3rd Edition., John-Wiley & Sons, New York, 239 p.

Masuda, A., and Ikeuchi, Y., 1979. Lanthanide tetrad effect observed in marine environment. Geochem. J., 13, 19–22.

Masuda, A.; Kawakami, O.; Dohmoto, Y., and Takenaka, T., 1987. Lanthanide tetrad effects in nature: two mutually opposite types, W and M., Geochem. J., 21, 119–124.

Middlemost, E. A. K., 1975.The Basalt Clan. Earth Science Reviews, 11, 337-364.http://dx.doi.org/10.1016/0012-8252(75)90039-2

Nasr, B.B., and Youssef, M., 1995. New occurrences of Tertiary alkaline rocks at Gebel Elba area South Eastern Desert, Egypt. Ann. Geol. Surv., XX. , 871 – 873.

Pearce, J. A.; Harris, N.B., and Tindle, A.G., 1984. Trace element Discrimination diagrams for the tectonic interpretation of granitic rocks. J. Petrology, 25 , 956 – 984.

Rollinson, H., 1993. Using Geochemical Data: Evaluation, Presentation, Interpretation. Longman Scientific Technical, 133–142.

Schilling, J. G., 1975. Rare-earth variations across "normal segments" of the Raykjanes Ridge, 60–53°N, Mid-Atlantic Ridge, 29°S, and East Pacific Rise, 2–19°S, and evidence of the composition of the underlying low-velocity layer. J. Geophys. Res., 80, 1459–1473.

Serencsits, C. M.; Faul, H.; Foland, K. A.; Hussein, A. A., and Lutz, T. M., 1981.Alkaline ring

complexes in Egypt; their ages and relationship in time. J. geophys. Res, 84, 3009-3013.

Shahin, H. A. A., 2000. Geological, petrographical and geochemical studies of Gabal Elba area south Eastern Desert, Egypt, Ph. D. Thesis, Fac. Sci. Al- Azhar Univ., 220p.

Shahin, H. A. A., 2014. Zr-Y-Nb-REE mineralization associated with microgranite and basic dykes at EL Sela shear zone, south Eastern Desert, Egypt.Springer Plus, 3, 573.

Shaw, D. M., 1968. A review of K/Rb fractionation trends by covariance analysis. Geochim. Cosmo-chim., Acta, 32, 573-601.

Shellnutt, J.G., and Zhou, M.-F., 2007. Permian peralkaline, peraluminous and metaluminous A-type granites in the Panxi district, SW China: their relationship to the Emeishan mantle plume. Chem. Geol., 242, 286–316.

Shellnutt, J.G.; Zhou, M.-F. , and Zellmer, G.F., 2009a. The Permian Baima Igneous Complex (SW China): the role of Fe-Ti oxide crystallization in the formation of A-type granitoids with implication for the Daly gap. Chem. Geol., 259, 204–217.

Takla, M.A.; Basta, E.Z.; El-Sharkawi, M. A., and Fawzie, E.,1976. The mineralogy of some wolframite veins from Egypt. Bull., Fac. Sci., Cairo Univ, No. 49.

Taylor, S. R., 1965. The application of trace element data problems in petrology. In: Physical and chemical of the earth (Ahrens, L.H., Press, F., Runcor, S.R. and Urey, H. C. , Eds), 133-213.

Vail J.R., 1985a. Alkaline ring complexes in Sudan. J. Afr. Earth Sci., 3, 51-59.

Vail J.R., 1990. Geochronology of the Sudan. Overseas Geology and Mineral Resources, 66, 58p.

Zhao, Z. H., 1988. REE tetrad effects—an important indicator for fluid/melt interaction. Proc. 3rd Congress on Mineralogy, Petrology and Geochemistry of China, 47–49 (in Chinese with English abstract).

Zhao, Z. H., 1992. Petrogenetic models of crust-type and crust-mantle type granitoids as evidenced by REE patterns. In: Petrogenesis and Mineralization of Granitoids (Tu, Guang-zhi, Xu, Keqin and Qiu,Yuzhuo, Eds.), 54–65, Science Press, Beijing.

—————

جيولوجية وكيميائية واشعاعية معقدة جبل شنديب القلوية، جنوب الصحراء الشرقية، مصر

حسن عبد الرازق شاهين   و مسعود صلاح مسعود

تكون معقدة جبل شنديب من الوحدات الصخرية على شكل نتوء دائرى طبوغرافية عالية.

هذه المعقدة يبلغ قطرها حوالى ١٢ كيلومتر قاطعة الصخور البركانية القديمة وضخور التوناليت –جرانوديورايت. تتكون هذه المعقدة من صخور الجابرو الحديث و صخور الجرانيت القلوى وصخور السيانيت القلوى وبقايا الصخور البركانية التى يمثلها صخور التراكيت وصخور الريوليت. هذه الصخور القلوية تظهر ثراء كبير فى بعض المعادن النادرة مثل الزركون الذى يصل الى ٤٥٢٧ جزء فى المليون و النيوبيم الذى يصل الى ٧١٧ جزء فى المليون والاتريوم الذى يصل الى ٨٠٦ جزء فى المليون والعناصر الارضية النادرة مثل عنصرلانثانوم الذى يصل الى ٥٥٣ جزء فى المليون وعنصر السيريوم الذى يصل الى ١٥٨١ جزء فى المليون

وعنصرالبراسوديميوم الذى يصل الى ٢١٤ جزء فى المليون وعنصرالنيوديميوم الذى يصل الى ١١٤٥ جزء فى المليون وعنصر الساماريوم الذى يصل الى ٢٩٩ جزء فى المليون وعنصرالگادولينيوم الذى يصل الى ٥٥ جزء فى المليون وعنصر الديسبروسيوم الذى يصل الى ٨٥ جزء فى المليون. ارتفاع نسبة Rb/Sr وانخفاض نسبة Ba/Rb فى الصخور القلوية لمعقدة جبل شنديب اظهر ارتفاع درجة عمليات التبلور الجزئى المصاحبة للصهير. أظهرنمط توزيع العناصر الارضية النادرة ان الصخور القلوية لمعقدة جبل شنديب تتميز بوجود M-type and W-type tetrad effect. تفاعل المحاليل فى الصهير فى المراحل الاخيرة من التبلور الجزئى اشار الى من اهم العوامل المتحكمة فى تكوينREE tetrad effects فى هذه الصخور القلوية. أهم المعادن الحاملة للعناصر الارضية النادرة هى الزيركون و الزونيتيم والمونازيت والالانيت والاباتيت. كذلك من المعادن الثانوية التى وجدت هى الكولومبيت و اليورانوفين واليورانوثوريت والتيتانيت. اظهرت القياسات الحقلية الاشعاعية والتحاليل الكيميائية انخفاض محتوى اليورانيوم للصخور الجرانيت والسيانيت القلوية لمعقدة جبل شنديب. يصل المستوى الاشعاعى فى صخور الجرانيت القلوى الى ١٣,٧٠ جزء فى المليون بينما يصل الى ٤,٩٠ جزء فى المليون فى صخور السيانيت القلوى. اظهرت التحاليل الكيميائية ان محتوى اليورانيوم فى صخور الجرانيت القلوى يصل الى ٣٥ جزء فى المليون بينما يصل الى ١٥ جزء فى المليون فى صخور السيانيت القلوى.